In Situ Formation of Lead Phosphates in Soils as a Method to Immobilize Lead

3 AUTHORS:

Michael V. Ruby
Integral Consulting, Inc.
40 PUBLICATIONS **2,909** CITATIONS

SEE PROFILE

Andy Davis
Geomega
62 PUBLICATIONS **2,741** CITATIONS

SEE PROFILE

Andrew Nicholson
Integral University
9 PUBLICATIONS **457** CITATIONS

SEE PROFILE

In Situ Formation of Lead Phosphates in Soils as a Method to Immobilize Lead

Michael V. Ruby, * **Andy Davis, and Andrew Nicholson**

PTI Environmental Services, 2995 Baseline Road, Suite 202, Boulder, Colorado 80303

Considerable evidence, both theoretical and experimental, supports the assertion that lead phosphates are the most stable environmental soil lead form and that they may form rapidly when adequate phosphate is present. This study demonstrated that the weathering of galena to insoluble lead phosphates in soils at a port facility historically used for shipment of ore concentrates is due to the presence of adequate soil phosphate. Geochemical modeling indicated that the addition of a phosphate amendment to Pb-bearing soil would result in lead phosphate formation with an estimated aqueous lead solubility of 0.1 $\mu g/L$ in soil. Assessment of the potential lead bioavailability from ingestion of pyromorphite, which will be controlled by lead mineral dissolution in the acidic environment of the human stomach, indicated limited bioaccessibility of lead. The study results suggest that in situ lead stabilization through phosphate amendment may provide a cost-effective method for reducing the leaching, migration, and bioavailability of lead from soils.

Introduction

The environmental dissolution and migration of lead (Pb) in soils is dependent on the solubility of the original Pb-bearing solids, the formation of secondary alteration (weathering) products and their solubility, and the soil matrix geochemistry [water content, pH, percent clay, amorphous ferric and manganese hydroxides, and permeability (1)]. The form and migration of Pb have become important issues at Pb-impacted sites, especially during the establishment of remedial cleanup goals. Therefore, induced alteration of primary Pb minerals to a less soluble form represents an attractive alternative for in situ stabilization and attenuation of Pb in soils. In addition, a lead mineral that is stable in the acidic environment of the human stomach will limit bioavailable lead, resulting in reduced human health risk.

Lead phosphates have been demonstrated to be the most stable environmental Pb form under a wide variety of conditions. The relative solubilities of simple Pb compounds (Table 1) indicate that lead phosphates are less soluble under equilibrium conditions than oxides, hydroxides, carbonates, and sulfates under earth-surface conditions. The solubility products for the pyromorphite mineral family [$Pb_5(PO_4)_3X$; X = halide or hydroxide], consisting of chloro-, bromo-, hydroxy-, and fluoropyromorphite, have been measured at $10^{-84.4}$, $10^{-78.1}$, $10^{-76.8}$, and $10^{-71.6}$, respectively (2–6), resulting in a thermodynamic stability sequence for lead pyromorphites of $Pb_5(PO_4)_3Cl$ > $Pb_5(PO_4)_3Br$ > $Pb_5(PO_4)_3OH$ > $Pb_5(PO_4)_3F$. In comparison, the solubility products of anglesite ($PbSO_4$), cerussite ($PbCO_3$), galena (PbS), and litharge (PbO) have been measured at $10^{-7.7}$, $10^{-12.8}$, $10^{-27.5}$, and $10^{+12.9}$, respectively (7, 8), indicating that lead pyromorphites are

considerably less soluble than the Pb phases generally found in ore materials [galena, anglesite, and cerussite (9)], paint (basic lead carbonate [$2PbCO_3\cdot Pb(OH)_2$]), litharge (10), and those believed to occur as a result of automobile emissions [anglesite, cerussite, and Pb adsorbed to soil surfaces (11–13)].

Equilibrium solubility studies of Pb in non-calcareous soils indicate that Pb concentrations are controlled by the formation of insoluble lead phosphates (14). Experiments conducted by Nriagu (6) indicated that in dilute phosphate solutions, lead halides are rapidly converted to pyromorphite and/or pyromorphite solid solutions. Recently, Ma et al. (15) demonstrated that the pyromorphite mineral family formed when soluble phosphorus (P) compounds, or apatite [$Ca_{10}(PO_4)_6(X)_2$; X = halide or hydroxide], were mixed with solutions of Pb. These data indicate that dissolution of apatite or addition of calcium phosphate can provide the necessary phosphate (PO_4) for the formation of insoluble pyromorphites (<15 $\mu g/L$ solubilized Pb at pH 5–7) and that, in the presence of elevated PO_4 activity, pyromorphite forms rapidly. In addition, kinetic studies of lead immobilization by hydroxyapatite in aqueous solutions (16) indicate that solutions containing approximately 100 mg/L Pb are reduced to <0.5 $\mu g/L$ Pb in under 10 min by the addition of finely divided hydroxyapatite. The reaction mechanisms are dominated by the dissolution of hydroxyapatite and the precipitation of hydroxypyromorphite and chloropyromorphite in Cl-free and Cl-containing solutions, respectively. On the basis of these theoretical and experimental lines of reasoning, the formation of lead phosphates appears capable of controlling soil Pb solubility, and it follows that a phosphate amendment may provide a method of Pb stabilization in soils.

Site Characteristics and Use. The subject site is a port facility, where galena ore concentrate and smelter dross arriving by rail were offloaded, stored, and reloaded onto seagoing vessels from 1974 through 1985. The Pb-bearing mine and smelter products transported through the port facility originated primarily in the "new lead belt" of south-central Missouri. Smelter dross is a byproduct of metal ore smelting, consisting of complex metal oxides (e.g., iron–copper–lead oxide), of native metals, and possibly of remnant sulfide minerals (17). Dross contains a high concentration of metals and is reused in the smelting process. A phosphoric acid plant borders the site to the north, and either the deposition of airborne P compounds or the storage and handling of high-P-content materials at the site has resulted in elevated soil P concentrations.

Weathering (Authigenic) Reactions in Soils. The orebodies in the "new lead belt" were formed at temperatures of 250–400 °C, at depths greater than 1 km, and contained galena as the primary Pb-bearing phase. Sulfide ore minerals are thermodynamically unstable when exposed to earth-surface conditions (decreased temperature, increased moisture content, and presence of oxygen), and alter to more stable mineral forms. The two basic

---

* To whom correspondence should be addressed.

Table 1. Theoretical Solubility and Concentration of Pb in Pb Phases

Pb phase	stoichiometry	$\log K_{sp}$	fraction Pb in each phase
litharge	PbO	12.9[b]	0.93[a]
anglesite	PbSO$_4$	−7.7[b]	0.68[a]
cerussite	PbCO$_3$	−12.8[c]	0.78[a]
galena	PbS	−27.5[h]	0.87[a]
chloropyromorphite	Pb$_5$(PO$_4$)$_3$Cl	−84.4[d]	j
hydroxypyromorphite	Pb$_5$(PO$_4$)$_3$OH	−76.8[e]	j
fluoropyromorphite	Pb$_5$(PO$_4$)$_3$F	−71.6[f]	j
bromopyromorphite	Pb$_5$(PO$_4$)$_3$Br	−78.1[f]	j
corkite	PbFe$_3$(PO$_4$)(SO$_4$)(OH)$_6$	−112.6[g]	j
drugmanite	Pb$_2$(Fe,Al)(PO$_4$)$_2$(OH)$_2$	NA[i]	j
hinsdalite	PbAl$_3$(PO$_4$)(SO$_4$)(OH)$_6$	−99.1[g]	j
plumbogummite	PbAl$_3$(PO$_4$)$_2$(OH)$_5$·H$_2$O	−99.3[g]	j
lead−metal sulfate	(Fe,Zn,Pb)SO$_4$	NA	0.14 ± 0.05 (n = 60)
iron−manganese−lead oxide	(Fe,Mn,Pb)O	NA	0.024 ± 0.009 (n = 9)
lead−metal oxides	(Fe,Al,Zn,Pb)O	NA	0.10 (estimated)

[a] Literature value (23). [b] Obtained from MINTEQA2 database (37). [c] Ref 7. [d] Ref 4. [e] Ref 3. [f] Ref 5. [g] Ref 2. [h] Ref 8. [i] NA = not available. [j] 0.67 ± 0.10 (n = 25), all lead phosphates.

alteration mechanisms involve either transformation of the parent mineral to a related chemical species (incongruent alteration, which results in pseudomorphic products) or dissolution of the primary mineral phase in infiltrating rainwater, and reprecipitation of secondary phases [congruent alteration (18)]. In general, sulfide minerals will weather to hydrated oxides, sulfates, phosphates, and carbonates, depending on the soil pH and availability of soil anions (8, 18).

The weathering and transformation of parent minerals formed under high temperature and pressure to minerals that are stable under low temperature and pressure is a slow process, dependent primarily on the stability of a mineral phase and the climate [e.g., sulfide minerals may start to oxidize in <1 year, whereas many silicates require 20 years for initiation of alteration (18)]. Mineral dissolution rates are controlled by several factors, including the crystallinity of the parent mineral, the activity of ionic species and their diffusion rates in the soil, the rate of diffusion of oxygen into the soil, the rate of hydrolysis of ions at the surface of the minerals, and the soil pH. Therefore, thermodynamically unstable phases may persist in the soil for extended periods of time if a combination of the above parameters results in slow alteration rates. Because many transformation reactions in soils are kinetically controlled, metastable and poorly crystalline phases are common, indicating that the reactions in soils have not yet reached equilibrium (18).

Much of the current geochemical literature indicates that oxides and carbonates are the stable forms in which base metals, such as Pb, copper (Cu), or zinc (Zn), are likely to occur in aerobic environments. However, predictions based on thermochemical data suggest that the formation of base metal phosphates will also be important in the fixation of base metals in soils and sediments (2). Phosphorus is present at an arithmetic mean concentration of 400–600 mg/kg in U.S. soils (8, 19) and is frequently associated with organic material (18). Therefore, although the formation of insoluble lead phosphate minerals is predicted to control the aqueous solubility of Pb (2), a lack of available soil phosphorus may preclude their formation.

Formation rates of phosphate minerals at earth-surface conditions are difficult to predict; however, hydroxy- and chloropyromorphite precipitate from aqueous solutions containing Pb [(as PbCl$_2$, Pb(NO$_3$)$_2$, or Pb(CH$_3$CO$_2$)$_2$] and hydroxyapatite in less than 10 min between pH 5 and 7 (15, 16). Although mineral formation rates will be slower in a soil environment than in an aqueous laboratory experiment, optimization of soil parameters (e.g., soluble phosphate concentration, water content, and degree of mixing) is likely to yield rapid production of pyromorphite. The objective of this paper is to evaluate the formation, stability, and potential bioaccessibility of lead phosphates in the soils at the port facility and to propose a method for *in situ* immobilization of Pb in soils, based on geochemical modeling of lead phosphate formation.

Methods

Seven composite surface soil samples (0–6 in.), from random locations across the port facility, were used in this study. Each sample was oven dried for 48 h at 80 °C and sieved to <250 μm. This size fraction facilitates reproducible bulk lead analysis by X-ray fluorescence (XRF) and yields representative point counts during electron microprobe analyses. Total Pb, iron (Fe), and manganese (Mn) concentrations were measured in each sample by XRF, and phosphorus concentrations were measured by nitric acid digestion (EPA Method 3050; ref 20) and analysis by inductively coupled plasma (ICP, EPA Method 6010; ref 20). The use of ICP for P analyses was necessitated by the difficulty in determining accurate P concentrations by XRF. Available phosphate from each sample was determined by de-ionized water extraction (21) with measurement by ion chromatography. Available chloride was also measured in the water extracts. Sample pH values were determined by the saturated paste method (21). Results from the independent collection and analysis of 10 surface samples (0–6 in.) were used to assess data quality.

Sample preparation and electron microprobe analysis (EMPA) were conducted at the Laboratory for Geological Studies, University of Colorado at Boulder, on a JEOL 8600 electron microprobe by the method reported in ref 22. The confirmatory EMPAs (10 samples) were conducted at RJ Lee Group, Inc. (Monroeville, PA) using a CAMECA CAMEBAX microprobe and similar operating parameters. The confirmatory samples were analyzed only for the relative occurrence of Pb phases, Pb-bearing

particle sizes, and Pb phase associations and were not analyzed for bulk metals, pH, or lead phosphate chemistry, as was done with the primary sample set. Lead phase associations were recorded for each grain and were defined as (1) cemented—Pb phases bound together by non-Pb-bearing phases, and non-Pb-bearing phases bound together by Pb phases; (2) liberated—Pb phases free from any matrix; (3) enclosed—Pb phases completely surrounded by a primary mineral phase (e.g., silicate or sulfide mineral) or by an alteration or precipitation reaction material; and (4) rinding—a secondary Pb phase that is rinding a primary Pb phase.

The grain size of each Pb carrier was determined by measuring the long-axis dimension (μm), and the weight percent (wt %) of Pb in those phases with variable Pb concentrations was measured in a representative number of grains [10–60 analyses, depending on the homogeneity of each phase (Table 1)]. The Pb mass distribution in each sample was determined by summing the long-axis measurements for each phase, multiplying by lead concentration (measured) and specific gravity (literature values) (23), and normalizing the resultant mass distribution numbers to 100%. Finally, the chemistry of lead phosphates was determined using quantitative analyses by wavelength dispersive spectrometry (WDS) on 25 randomly selected particles.

Because the chemical composition of lead phosphates, determined by electron microprobe, does not verify the presence of a discrete crystalline structure, physical separation techniques were combined with X-ray diffraction (XRD) to isolate and identify lead phosphates. To isolate the lead phosphates present in the port facility samples, a combination of density, magnetic, and solubility-based separations was employed to separate the lead phosphate minerals from the bulk soil matrix and the Pb phases other than lead phosphates (e.g., anglesite, galena, and cerussite).

Samples SS-41 and SS-49 were sieved to <74-, 74–125-, 125–250-, and >250-μm particle size fractions. The 74–125- and 125–250-μm fractions of samples SS-41 and SS-49 were combined to provide approximately 30 g of each preseparation sample for the heavy mineral separations. These particle size distributions were chosen because particles <74 μm tend to agglomerate, while particles >250 μm will not pass through the stopcock of the separatory funnel. Each composite sample was added to a 500-mL separatory funnel containing approximately 250 mL of acetylene tetrabromide (specific gravity of 2.96 g/cc at 25 °C). The particles with specific gravities greater than 2.96 g/mL were separated, washed with acetone, and dried. This process separates Pb phases and other heavy minerals from the bulk of the soil matrix (silicates, organic fraction).

Magnetite was removed with a hand magnet, and the remaining sample material was passed through a Frantz isodynamic separator at 1.5 A with a track tilt of 10° toward the electromagnet. A portion of the nonmagnetic material was ground to approximately 1 μm and examined by XRD to identify Pb minerals using a Scintag X-ray diffractometer with Cu K-α radiation at 40 kV and 35 mA. The samples were continuously scanned over a 2θ of 2–60°, with data collected in 0.02° increments. Samples were prepared as slurry mounts on glass slides due to the small sample size.

Because anglesite has a well-defined cleavage pattern, the crushed anglesite particles have a preferred orientation in the slurry mount, resulting in an intense powder pattern for anglesite. In contrast, the lead phosphates have no preferential orientation in the mount, resulting in a weak diffraction pattern. Therefore, a sample containing even a minor concentration of anglesite generates a strong anglesite diffraction pattern, obscuring the peaks that may be present from lead phosphates. Because lead phosphate diffraction lines could not be distinguished against the background of the anglesite diffraction pattern in either the 75–125- or the 125–250-μm nonmagnetic fractions, anglesite was dissolved from the sample as follows.

The remaining material from the 75–125- and 125–250-μm size fractions, both magnetic and nonmagnetic, was combined into a single sample. The magnetic separator was run at 0.6 and 1.5 A to separate the sample into three fractions (nonmagnetic, semimagnetic, and magnetic). The nonmagnetic and semimagnetic fractions (approximately 0.2 g) were each placed in 2-L polyethylene bottles, and 2 L of deionized water, adjusted to pH 10.0 with NaOH, was added. The bottles were rotated end-over-end for 30 h (final pH of 10.2), and the contents were filtered through Whatman No. 1 filter paper. The insoluble material (approximately 0.1 g in each bottle) was washed with acetone, oven-dried, and examined by XRD for Pb phases, resulting in the identification of lead phosphate mineral phases.

Results

Soil Parameters. Measured soil pH values varied widely across the port facility, ranging from 4.2 to 7.4 (Table 2). Samples with pH values >6.0 contained visible shell fragments, most likely providing buffering capacity to the soil.

The XRF results indicate that Pb in the port facility samples varied from 110 to 183 000 mg/kg (Table 2). Measured phosphorus concentrations ranged from 1400 to 17 700 mg/kg (arithmetic mean of 5360 mg/kg, Table 2), considerably above the average P concentration in U.S. soils [600 mg/kg (8)], possibly due to storage and handling of P-containing materials at the site or deposition of airborne P from the phosphoric acid plant bordering the site to the north. Because the average P concentration in the port facility soil is 9 times greater than the average U.S. soil, this soil contributes the required phosphate activity necessary for the formation of end-member lead phosphate minerals.

Iron and Mn concentrations were determined by XRF (Table 2), because Pb in soils is often present as iron–lead oxides and manganese–lead oxides (24, 25), and the presence of manganese–lead oxides, the formation of which may be controlled by Mn concentrations (22), has been observed to decrease the solubility of Pb in soils (26). Arithmetic mean Fe and Mn concentrations in the port facility soils were 2.5 ± 1.6% and 180 ± 80 mg/kg, respectively. Both these values fall within the normal range of approximately 3.8% and 20–3000 mg/kg for Fe and Mn, respectively, observed in surface soils in the United States (8, 27).

Determination of available phosphate yielded results that were initially confounding (Table 2) but were confirmed with repeated analyses. The lack of available PO$_4$ (detection limit = 1 mg/kg on dry sample weight basis) in the water extracts was interpreted as an indication that dissolution of excess Pb and formation of lead phosphates

Table 2. Soil Parameters and Pb Mass Distribution of Port Samples

lead phase (%)	SS-15	SS-29	SS-41	SS-49	SS-51	SS-80	SB-3	av Pb mass distribution (%) in PTI samples	av Pb mass distribution (%) in RJ Lee samples[a]
lead phosphates (chemistries in Table 1)	17	29	88	41	75	60	16	46[b] (44–48)[c]	40
anglesite, PbSO$_4$	3	35	12	44	7	13	56	24 (22–26)	25
galena, PbS	66	18		15	6	26	28	23 (20–24)	25
cerussite, PbCO$_3$	14				11			4 (3–5)	7
lead–metal sulfate, (Pb,M)SO$_4$[d]		19		tr				3 (1–5)	1
iron–manganese–lead oxide (Fe,Mn,Pb)O[e]	tr[m]				1			tr	tr
Pb metallics (Pb,M)O[f]		tr		tr		1		tr	1
no. of grains counted	172	186	170	260	105	108	208	av value	
sample pH[h]	7.4	4.7	6.3	5.8	7.2	4.2	6.0		
lead (mg/kg)[i]	10 200	13 300	6 600	183 000	3 600	1 900	127 000	43 200 (70 700)[g]	
phosphorus (mg/kg)[j]	4 770	3 060	3 850	5 000	1 400	1 730	17 700	5 360 (5 620)[g]	
H$_2$O avail. PO$_4$ (mg/kg)[k]	<1[l]	<1	1.1	4.0	<1	<1	<1		
H$_2$O avail. Cl$^-$ (mg/kg)[k]	730	34	19	34	17	21	14	124 (267)[g]	
iron (wt %)[i]	1.5	5.9	1.7	1.2	2.0	1.1	2.6	2.5 (1.6)[g]	
manganese (mg/kg)[i]	280	190	140	110	200	70	320	180 (80)[g]	

[a] Average Pb mass distribution for set of 10 samples analyzed by RJ Lee Group, Inc. (Monroeville, PA). [b] Average mass of Pb in phase calculated across entire set of samples. [c] 90% confidence interval calculated from Mosimann (38). [d] Lead–metal sulfate consists of Fe, Zn, and Pb as sulfate mineral phase. [e] Iron–manganese–lead oxide contains varying metal concentrations in the relative ratio Fe > Mn > Pb. [f] Lead metallics are oxidized solid solutions of Pb combined with other metals, generally Fe, Al, and Zn. [g] Standard deviation on mean value for parameter measured. [h] Determined by the saturated paste method (21). [i] Determined by X-ray fluorescence. [j] Determined by digestion and ICP analysis. [k] Reported on dry sample weight basis. [l] Detection limit of 1 mg/kg PO$_4$ (on dry sample weight basis) for extracts by ion chromatography. [m] tr = <0.5% of crystalline Pb mass in sample.

during the extraction procedure had removed the soluble PO$_4$ from solution. The water-soluble chloride (range of 14–730 mg/kg, average of 124 mg/kg) is consistent with average chloride concentrations in U.S. soils [100 mg/kg (8)], although the elevated concentration in SS-15 indicates that proximity of the site to the ocean may have resulted in elevated Cl$^-$ concentrations due to ocean aerosols (28).

Lead Mineralogy. The cumulative Pb mass distribution (or Pb pool), based on mineralogy in the port facility samples, was lead phosphates > anglesite > galena > cerussite > lead–metal sulfate, iron–manganese–lead oxide, lead metallics, in both the initial and confirmatory samples (Table 2). The lead–metal sulfate contains Fe, Zn, and Pb as a sulfate mineral, while the iron–manganese–lead oxide contains varying concentrations of Fe, Mn, and Pb, in the relative ratio Fe > Mn > Pb. The lead metallics are oxidized solid solutions of Pb with Fe, Al, and Zn.

Cerussite was present only in samples SS-15 and SS-51, which had soil pH values of 7.4 and 7.2, respectively, whereas the soils with pH values ranging from 4.2 to 6.3 generally contained more anglesite (Table 2). This observation is consistent with the predicted formation of cerussite and anglesite at soil pH values greater and less than 6.5, respectively (8). The concentration of P in each sample does not vary linearly with the observed percent mass of lead phosphate (r = 0.28). Multiple P-bearing compounds may be present in the soils, not all of which are soluble, and can yield PO$_4$ for the formation of lead phosphates, resulting in a situation where bulk P concentration would not necessarily be related directly to the occurrence of lead phosphates.

The Pb mass distribution determined for the confirmatory set of 10 samples varies by ±6%, for any Pb phase, from the results of the primary data set (Table 2). These data indicate that independent sample collection and EMPA produced nearly identical results for sets of 7–10 samples at this site, thereby validating the EMPA meth-
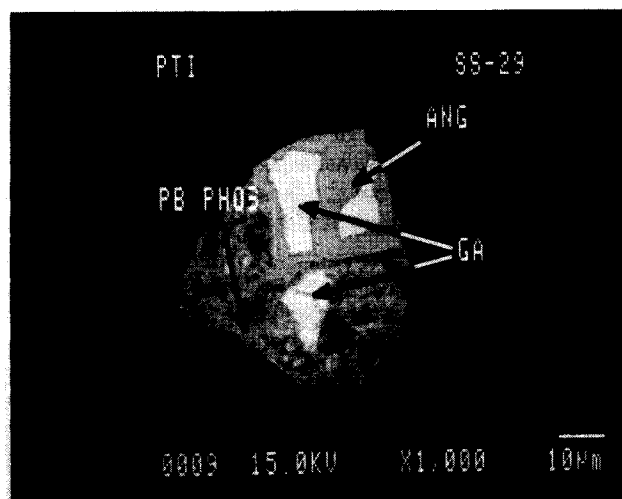

Figure 1. Photomicrograph of a galena crystal altering to anglesite, followed by alteration to lead phosphate. The original cubic crystal of galena is preserved in the anglesite alteration product.

odology and the representativeness of the seven samples collected and analyzed for this study.

Lead mineral associations observed in the port facility samples indicate that galena particles were either liberated (52% of galena particles) or enclosed in lead phosphate (28%), anglesite (18%; Figure 1), or cerussite (2%; Figure 2). Anglesite generally occurred as liberated particles (90% of anglesite particles) and was occasionally rinded by lead phosphate (8%; Figure 1) or lead–metal sulfate (2%). Cerussite was generally liberated (88% of cerussite particles), with occasional grains either rinded (9%; Figure 2) or cemented (2%). Lead phosphate grains occurred as liberated particles (62%), with the remainder rimming other Pb-bearing particles (20%, after galena, anglesite, and cerussite; Figures 1–3) and non-Pb-bearing particles of quartz, feldspar, pyrite, and coal (18%, Figure 4). These
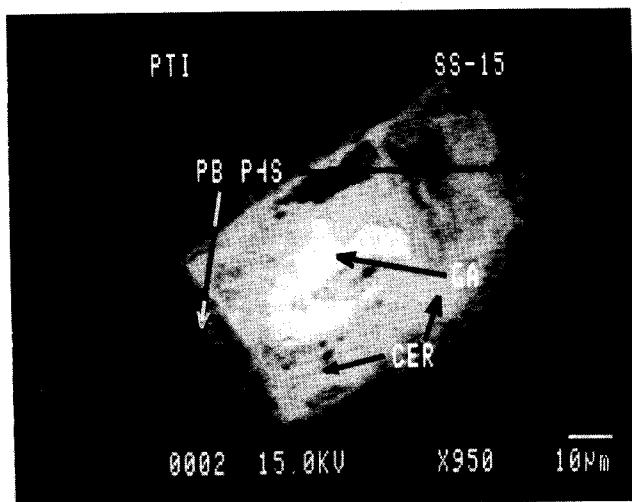
Figure 2. Photomicrograph of galena altering to cerussite, followed by alteration to lead phosphate. The original cubic crystal of galena is preserved in the cerussite alteration product.
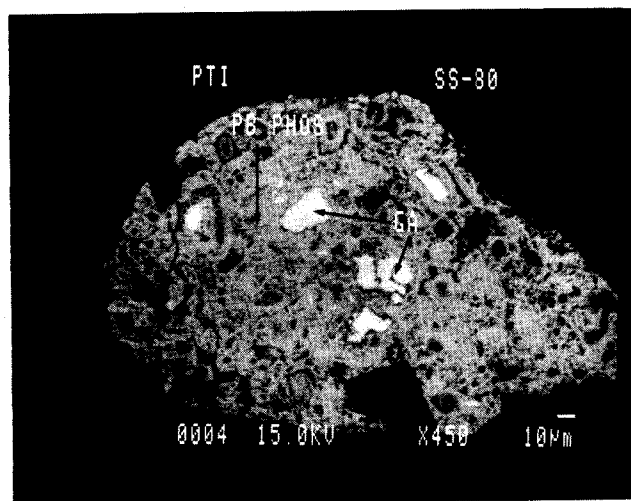

Figure 3. Photomicrograph of galena grains altering directly to lead phosphate.

Pb mineral associations suggest that the primary Pb mineral transported to the site, galena, altered initially to anglesite or cerussite, depending on the soil pH, and subsequently to lead phosphate (Figures 1 and 2). The oxidation products $PbSO_4$ and $PbCO_3$ (Figures 1 and 2) are often pseudomorphs after galena, indicating incongruent alteration. Formation of the ubiquitous lead phosphate phases in the port facility samples most likely involves their precipitation directly from the soil–water solution (congruent alteration, Figures 1–4). The coating of soluble Pb phases (galena, anglesite, and cerussite) with lead phosphate reaction rinds will reduce their solubility in the site soils.

Quantitative analyses by microprobe using WDS were performed on 25 randomly selected lead phosphate grains, representing 18% of the lead phosphate grains analyzed in the initial analysis (Table 3). These analyses indicate that F^- may substitute for Cl^-, resulting in formation of fluoropyromorphite (samples SS-15 and SS-51; Table 3); and that Ca^{2+} and SO_4^{2-} may substitute for Pb^{2+} and PO_4^{3-}, respectively, resulting in apatites and the corkite/hindsdalite family minerals. Fe was present occasionally, indicating alteration toward corkite or drugmanite-type minerals, while Si, Al, and Mn were uncommon substituents in the lead phosphates.
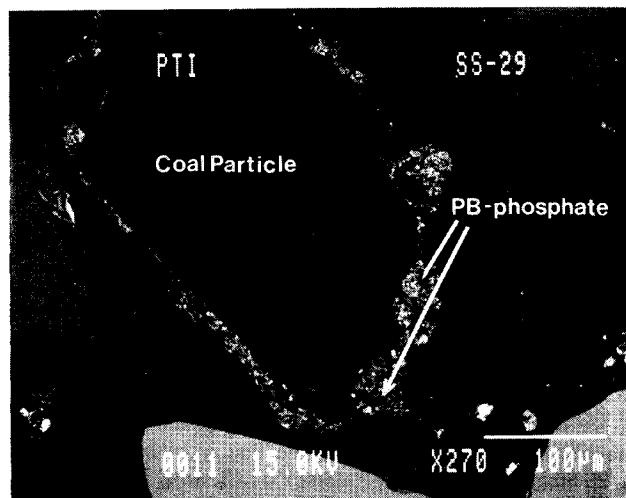

Figure 4. Photomicrograph of lead phosphate precipitate on a grain of coal.

The results of the quantitative analyses were plotted on a ternary diagram (Figure 5) by normalizing the percent weights of the three constituents (Pb, P, and S, as oxides) to 100% and plotting the locations of the lead phosphate particles in PbO, SO_3, and P_2O_5 space. The points that plot in discrete fields can then be compared with known percent compositions of the common lead phosphates. The shaded fields that correspond to lead phosphate minerals include approximately 4% change in percent composition from the exact mineral formula to allow for analytical errors and for the presence of minor impurities (Figure 5).

The quantitative analyses performed on sample SB-3 (Figure 5, □) indicate that most of the lead phosphate grains in this sample are composed of pyromorphite $[Pb_5(PO_4)_3Cl]$, whereas the lead phosphates in sample SS-80 are closely grouped within the drugmanite $[Pb_2(Fe,-Al)(PO_4)_2(OH)_2]$ field (Figure 5, O). Chloropyromorphite has very low solubility under environmental conditions $[\log K_{sp} = -84.4\ (2)]$, and although $\Delta G°_f$ for drugmanite has not been determined, it is likely to have a similarly low solubility. The remaining lead phosphates are closely related to pyromorphite and drugmanite containing excess S (Figure 5) and are therefore classified as solid-solution mixtures within the pyromorphite–drugmanite–corkite series. Finally, the lead phosphate grain with approximately 55 wt % PbO (Figure 5, △) contains a chemical formula representative of the mineral plumbogummite $[PbAl_3(PO_4)_2(OH)_5\cdot H_2O, \log K_{sp} = -99.3\ (2)]$.

Because the majority of the lead phosphate analyses fall within the pyromorphite field, this phase appears to be the predominant lead phosphate forming at the site. These findings are consistent with those of Nriagu (2) and Cotter-Howells and Thornton (29), who predicted that pyromorphite would be the predominant lead phosphate in soils; they contrast, however, with the observations of Davis et al. (22), which indicated the formation of a lead phosphate solid solution in a mine-waste soil. The lack of a pyromorphite or other end-member lead phosphate forming in the mine-waste soil appears to have been due to limitations on PO_4 activity, precluding formation of end-member lead phosphates. In addition, these data appear to be in agreement with the experimental results of Santillan-Medrano and Jurinak (14), who observed a solid solution of mixed composition, interpreted to consist of $Pb_5(PO_4)_3OH$, $Pb(OH)_2$, and $Pb_3(PO_4)_2$, in soil solutions

Table 3. Results from Quantitative Analyses of Lead Phosphates in Port Facility Samples

sample no.	PbO[a]	P$_2$O$_5$	SO$_3$	FeO	SiO$_2$	Al$_2$O$_3$	MnO	F	Cl	CaO	total
SS-15/51	57.44	14.56	5.00	1.47	0.47	0.32	0.05	6.15	2.45	9.10	97.01
SS-15/51	68.41	11.70	1.97	4.62	0.15	0.11	0.02	4.55	1.83	4.44	97.80
SS-15/51	50.84	12.96	6.18	3.38	3.40	2.51	0.00	5.52	2.31	8.62	95.72
SS-15/51	67.39	13.81	3.08	1.19	3.47	0.93	0.01	5.12	2.43	2.03	99.46
SS-29	56.84	13.52	4.55	2.42	3.76	0.55	0.03	0.38	1.82	3.64	87.51
SS-29	64.52	14.10	2.86	1.92	0.85	1.64	0.16	0.46	2.28	2.76	91.55
SS-41	66.78	17.88	3.40	0.35	0.12	0.36	0.06	1.05	1.42	8.44	99.86
SS-41	68.49	17.41	1.29	0.57	0.55	0.32	0.05	0.50	1.98	5.35	96.51
SS-41	65.80	14.42	4.30	0.37	0.12	0.34	0.02	0.91	1.38	6.75	94.41
SS-41	36.24	25.70	1.26	2.24	2.13	1.96	0.09	1.92	0.58	17.26	89.38
SS-41	70.17	14.67	1.27	1.02	0.99	0.86	0.15	0.91	2.22	0.74	93.00
SS-49	54.85	7.77	6.45	4.97	6.84	3.63	0.01	0.05	1.12	1.40	87.09
SS-49	55.47	11.37	1.55	2.80	0.30	0.11	0.01	0.28	1.78	0.84	74.51
SS-80	66.60	18.03	3.45	0.28	0.10	1.09	0.00	0.45	1.99	4.60	96.59
SS-80	59.48	16.09	2.36	5.84	0.23	0.99	0.03	0.35	2.43	1.42	89.22
SS-80	70.55	18.46	2.25	0.71	0.10	0.70	0.05	0.57	2.17	1.76	97.32
SS-80	72.12	17.12	2.29	0.44	0.22	0.37	0.05	0.24	2.96	4.56	100.37
SB-3	75.77	14.59	2.48	0.46	0.04	0.10	0.00	0.33	2.34	1.33	97.44
SB-3	73.77	11.72	4.90	0.34	0.02	0.10	0.02	0.28	1.89	0.90	93.94
SB-3	77.38	14.19	2.01	0.20	0.05	0.06	0.05	0.18	2.89	1.15	98.16
SB-3	77.07	14.89	1.17	0.14	0.13	0.17	0.00	0.44	2.51	1.41	97.93
SB-3	79.22	15.37	0.90	0.20	0.00	0.03	0.01	0.21	2.69	0.33	98.96
SB-3	73.96	11.09	3.39	0.42	2.44	1.21	0.04	0.80	2.31	0.97	96.63
SB-3	75.62	15.86	1.13	0.26	0.07	0.14	0.01	0.35	2.70	1.30	97.44
SB-3	77.56	15.93	1.46	0.26	0.01	0.08	0.00	0.27	2.43	1.16	99.16

[a] All results reported as wt % of the given element oxide in the lead phosphate grain.

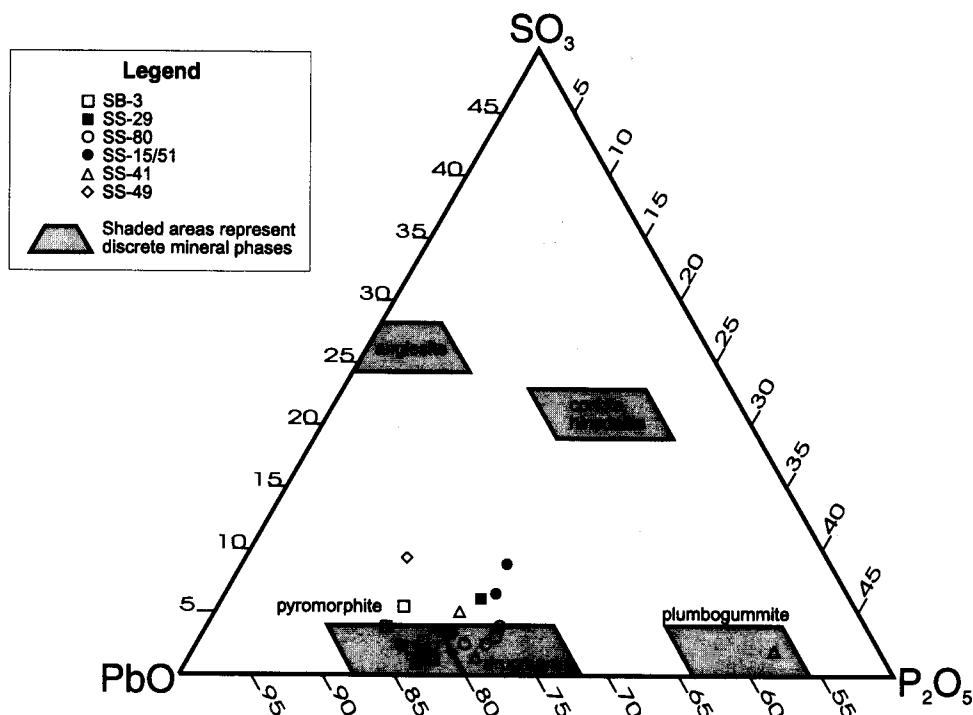**Figure 5.** Ternary diagram of the lead phosphate quantitative analyses at the port facility. Data for Pb, S, and P as oxides (PbO, SO$_3$, and P$_2$O$_5$), normalized to 100% of total weight.

with pH values >6.6. The absence of Cl$^-$ in their experiments precluded the formation of Pb$_5$(PO$_4$)$_3$Cl.

XRD. The XRD patterns obtained from the nonmagnetic 75–125- and 125–250-μm size fractions with specific gravities greater than 2.96 g/mL were identified as pure anglesite. However, subsequent to the dissolution separation, which was designed to selectively dissolve anglesite, the Scintag search/match program identified chloropyromorphite [Pb$_5$(PO$_4$)$_3$Cl] in both the nonmagnetic and semimagnetic fractions, while corkite [PbFe$_3$-(PO$_4$)(SO$_4$)(OH)$_6$] was identified in the nonmagnetic fraction. The presence of Fe-bearing corkite in the

nonmagnetic fraction may be due to insufficient Fe in the corkite to be separated at the voltage used with the magnetic separator. The removal of anglesite from the sample by dissolution, prior to successful XRD detection of the lead phosphates, verifies the theoretical solubility difference between lead phosphates and anglesite.

Reaction-Path Modeling (EQ3/6). Geochemical modeling was conducted using the reaction-path software package EQ3/6 (30) to determine the optimum theoretical phosphate necessary in the port facility soil to foster formation of lead phosphates. Reaction sequences were simulated by numerically "titrating" a mineralogy char-

Table 4. Input Parameters for EQ3/6 Modeling[a]

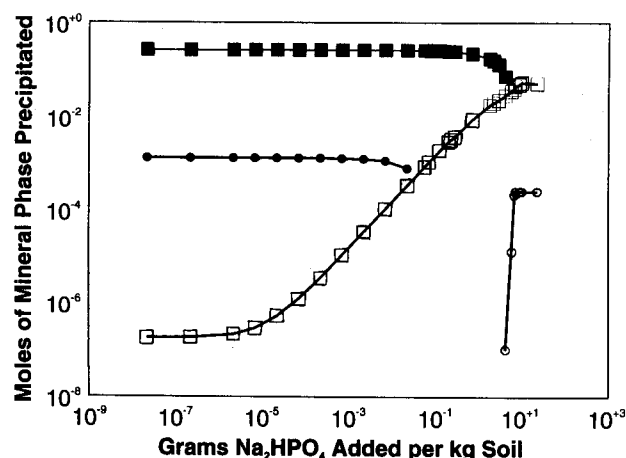| parameter	initial conditions
T (°C)	25
log P_{CO_2}	-2.0
log P_{O_2}	-0.7
galena (g/kg of soil)	10
hematite (g/kg of soil)	90
quartz (g/kg of soil)	650
calcite (g/kg of soil)	150
illite (g/kg of soil)	100

[a] Data source described in text.

Figure 6. Reaction path for port facility soils. (■) anglesite; (●) cerussite; (□) chlorophyromorphite, (O) plumbogummite. The precipitation sequence for the reaction is described in the text.

acteristic of port facility soils—containing 1% Pb (10 g/kg) as galena with solid disodium phosphate (Na_2HPO_4) and sodium chloride (10:1, Na_2HPO_4:NaCl by mass). The initial soil mineralogy (Table 4) was based on soil analyses from the county adjacent to the port facility (31). Thermodynamic values (log K) for litharge and plumbogummite were added to the EQ3/6 database. The reaction sequence was initiated with the solution speciation model EQ3 to simulate initial soil water (constant at 30% moisture) with trace amounts (<0.01 mg/L) of Al, Ca, P, Pb, and Si, and 5.9 mg/L NaCl (where Na^+ was used to balance the electrical charge). Log P_{O_2} and log P_{CO_2} were maintained at -0.7 and -2.0, respectively, representative of typical soil gas conditions (Table 4) (32, 8). The redox state of the system was fixed through equilibrium with atmospheric oxygen. Reaction progress (ξ), an incremental measure of the extent of reaction, was used to track the evolution of the computations.

Results from the reaction-path modeling (Figure 6) indicate that, prior to the addition of phosphate to port facility soil, cerussite (●) and anglesite (■) are the dominant stable lead-bearing phases in the soil. As disodium phosphate is added incrementally to the EQ3/6 model, cerussite is no longer a stable phase in the presence of 0.023 g of disodium phosphate/kg of soil (Figure 6). At 4.2 g of disodium phosphate/kg of soil, anglesite is no longer a stable lead phase, and all solid-phase lead is present as chloropyromorphite (□) and plumbogummite (O). The resultant pore water has a final pH of 6.6 and dissolved Pb of 0.12 µg/L. For comparison, the initial predicted soil pore water had a pH of 5.8 and Pb of 6500 µg/L. It was found that the addition of NaCl was necessary to avoid chloride limitations during chloropyromorphite formation.

Table 5. MINTEQA2 Modeling of Lead Dissolution under Stomach Conditions

pH	litharge, PbO (mg/L)	cerussite, PbCO3 (mg/L)	anglesite, PbSO4 (mg/L)	Cl-pyromorphite, Pb5(PO4)3Cl (mg/L)
1.5	5.9×10^{19}	5.7×10^6	150	80
2.0	1.2×10^{18}	1.7×10^6	74	18
4.0	1.6×10^{12}	2.0×10^3	49	0.38
6.0	3.9×10^7	23	49	0.01

These theoretical predictions are in agreement with the data of Xu and Schwartz (16), which indicated that the formation of chloropyromorphite from solutions of soluble Pb and hydroxyapatite would reduce aqueous Pb concentrations from 100 000 to <0.5 µg/L (detection limit).

Although these calculations do not account for the kinetic effects that control the rates at which galena will dissolve and chloropyromorphite will precipitate in soil, they demonstrate that amending 1 kg of soil containing 10 g of lead (1 wt %) as PbS with 4.2 g of Na_2HPO_4 (0.42 wt %) and 1.7 g of NaCl provides adequate phosphate and chloride to immobilize lead in the soil by the formation of chloropyromorphite.

The average P concentration in the port facility soils was 0.54 wt % (Table 2), corresponding to a maximum of 1.7 wt % as PO_4. Even if only 25% of this PO_4 is available (not verifiable using extraction methods due to the rapid formation of pyromorphite), the modeling results indicate that the average soil P concentration is adequate for inducing the formation of lead phosphates, thereby supporting the conclusions of the EQ3/6 modeling due to the observed formation of lead phosphates in the port facility soils.

Discussion

Recently, it has been recognized that Pb mineral solubility is an important factor controlling Pb bioavailability from mine-waste materials (29, 33). The solubility of ingested Pb phases is dependent on the mineralogy, the encapsulation of Pb phases within alteration and precipitation products, and the slow rates of Pb dissolution (kinetic constraints) that limit Pb bioaccessibility as the Pb-bearing solids traverse the gastrointestinal (GI) tract (34). Feeding studies in rats using lead phosphates are currently being conducted (35) to determine the bioavailability of ingested lead phosphates. Based on geochemical solubility constraints, lead phosphates should have limited solubility at pH values of 1.5–2 and 4–6, representative of the human stomach during fasting and fed conditions, respectively (36). To evaluate this hypothesis, the theoretical solubilities of litharge (PbO), cerussite, anglesite, and pyromorphite were evaluated at pH values of 1.5, 2.0, 4.0, and 6.0 using the equilibrium geochemical computer code MINTEQA2 (37; Table 5). The modeled results suggest that pyromorphite will be the least soluble of the Pb phases under both fasting and fed conditions. Based on the modeled results (equilibrium conditions), lead phosphates will be the least soluble Pb mineral form and should have limited solubility in the human stomach, especially under fed conditions, resulting in decreased concentrations of solubilized Pb available for absorption during passage through the small intestine. This discussion does not account for lead phosphate dissolution

kinetics, which may preclude steady-state conditions being attained during the approximately 2-h residence time of material in the human stomach (34). This factor may further reduce dissolved Pb concentrations available for absorption. Further study of this topic will indicate whether induced formation of lead phosphates will result in decreased Pb bioavailability from soils.

The Pb phosphate assemblage at the port facility is composed of sparingly soluble minerals [log K_{sp} = −84 to −113 (2)], of which chloropyromorphite and corkite were identified by XRD, and would produce less solubilized Pb under environmental soil conditions than the primary sulfide assemblage. Therefore, the alteration of PbS to lead phosphates results in enhanced environmental stability and reduced Pb dissolution into soil water or groundwater at the port facility. The formation of lead phosphates in any given port facility sample will be dependent on the presence of adequate P and counteranion (Cl^-, OH^-, F^-) activities. Although elevated concentrations of available PO_4 could not be verified using experimental methods, these results appear to verify the rapid formation of sparingly soluble lead phosphates. Based on the geochemical modeling conducted using EQ3/6, the addition of disodium phosphate (0.56 g) and NaCl (0.023 g) to a soil containing 10 g of Pb/kg of soil would result in the formation of chloropyromorphite and a reduction in dissolved Pb concentrations to approximately 0.1 μg/L. Addition of lime ($CaCO_3$) would also be desirable for acidic soils to achieve a pH value of approximately 7, at which pyromorphite formation rates are maximized (16) and solubility minimized (8). Additional work is necessary to delineate the pH and P activity relations that control the rate and extent of environmental lead phosphate formation. However, recent research indicates that crystalline chloropyromorphite will form rapidly (<10 min) from solutions of Pb and disodium phosphate or hydroxyapatite (15, 16) under laboratory conditions.

The presence of elevated Pb and P concentrations at the port facility, due to anthropogenic activity, indicates that lead phosphates have formed between the time that ore shipments were initiated (1974) and the termination of this activity (1985). Based on these dates, PbS that was deposited on the site soils has been present for a maximum of 19 and a minimum of 7 years (average residence time of 13 years). Forty-six percent of the original PbS has altered to lead phosphates in 13 years (Table 2), under uncontrolled environmental conditions, and it appears reasonable that this alteration rate could be increased by optimizing conditions (PO_4 and Cl activity, pH, water content, and mixing). Further study of this geochemical mechanism is necessary to determine whether P amendment will prove a viable means of Pb stabilization in soils. Theoretical evaluation suggests that the formation of lead phosphates will also reduce the bioaccessibility of Pb on ingestion, due to solubility constraints. Based on this research, the stabilization and reduced bioaccessibility of Pb suggest that P amendment may provide an appropriate remedial alternative for reducing Pb dissolution, migration, and exposure to potentially affected populations.

Literature Cited

(1) Chemical Attenuation Rates, Coefficients, and Constants in Leachate Migration; Electric Power Research Institute, Palo Alto, CA, 1984; p 14-1.
(2) Nriagu, J. O. Phosphate Minerals; Nriagu, J. O., Moore, P. B., Eds.; Springer-Verlag: New York, 1984.
(3) Nriagu, J. O. Inorg. Chem. 1972, 11, 2499–2503.
(4) Nriagu, J. O. Geochim. Cosmochim. Acta 1973, 37, 367–377.
(5) Nriagu, J. O. Geochim. Cosmochim. Acta 1973, 37, 1735–1743.
(6) Nriagu, J. O. Geochim. Cosmochim. Acta 1974, 38, 887–898.
(7) Wagman, D. D.; Evans, W. H.; Parker, V. B.; Schumm, R. H.; Halow, I.; Bailey, S. M.; Churney, K. L.; Nuttall, R. L. J. Phys. Chem. Ref. Data 1982, 11 (Suppl. 2), 392.
(8) Lindsay, W. L. Chemical Equilibria in Soils; John Wiley and Sons: New York, 1979; pp 328–341.
(9) Ridge, J. D., Ed. Ore Deposits in the United States 1933/1967; The American Institute of Mining Engineers: New York, 1968.
(10) Heaton, N. Outlines of Paint Technology; Charles Griffin and Co., Limited: London, England, 1940.
(11) Olson, K. W.; Skogerboe, R. K. Environ. Sci. Technol. 1975, 9 (3), 227–230.
(12) Biggins, P. D. E.; Harrison, R. M. Environ. Sci. Technol. 1980, 14, 336.
(13) Harrison, R. M.; Laxen, D. P. H.; Wilson, S. J. Environ. Sci. Technol. 1981, 15 (11), 1378–1383.
(14) Santillan-Medrano, J.; Jurinak, J. J. Soil Sci. Soc. Am. Proc. 1975, 39, 851–856.
(15) Ma, Q. Y.; Traina, S. J.; Logan, T. J. Environ. Sci. Technol. 1993, 27 (9), 1803–1810.
(16) Xu, Y.; Schwartz, F. W. J. Contam. Hydrol., in press.
(17) Drexler, J. W. Unpublished data. Department of Geological Sciences, University of Colorado at Boulder, 1993.
(18) Nahon, D. B. Introduction to the Petrology of Soils and Chemical Weathering; John Wiley & Sons, Inc.: New York, 1991; pp 1–48.
(19) Shacklette, H. T.; Boerngen, J. G. Element Concentrations in Soils and Other Surficial Materials of the Conterminous United States; U.S. Geological Survey Professional Paper 1270; United States Government Printing Office: Washington, DC, 1984.
(20) Test methods for evaluating solid waste. Volume 1A: Laboratory manual, physical/chemical methods; U.S. Environmental Protection Agency, Office of Solid Waste and Emergency Response: Washington, DC, 1986.
(21) Black, C. A., Ed. Methods for Soil Analysis. Part 2. Chemical and Microbiological Properties; American Society of Agronomy, Inc.: Madison, WI, 1965.
(22) Davis, A.; Drexler, J. W.; Ruby, M. V.; Nicholson, A. Environ. Sci. Technol. 1993, 27 (7), 1415–1425.
(23) Klein, C.; Hurlbut, C. S. Manual of Mineralogy; John Wiley & Sons, Inc.: New York, 1993; pp 334–550.
(24) McKenzie, R. M. Aust. J. Soil Res. 1980, 18, 61–73.
(25) Levy, D. B.; Barbarick, K. A.; Siemer, E. G.; Sommers, L. E. J. Environ. Qual. 1992, 21, 185–195.
(26) McKenzie, R. M. Aust. J. Soil Res. 1978, 16, 209–214.
(27) Kabata-Pendias, A.; Pendias, H. Trace Elements in Soils and Plants; CRC Press: Boca Raton, FL, 1984.
(28) Ericksson, E. Tellus 1955, 7, 243–250.

(29) Cotter-Howells, J.; Thornton, I. *Environ. Geochem. Health* **1991**, *13* (2), 127–135.

(30) Wolery, T. J.; Davekerm S. A. *EQ6: A Computer Program for Reaction Path Modeling of Aqueous Geochemical Systems: Users Guide and Documentation*; Lawrence Livermore National Laboratory, University of California: Livermore, CA, 1989.

(31) Hickman, G. L.; Owens, C. *Soil Survey of Mobile County, Alabama*; U.S. Department of Agriculture, Soil Conservation Service: Washington, DC, 1980; p 134.

(32) Krauskopf, K. B. *Introduction to Geochemistry*; McGraw-Hill: New York, 1979.

(33) Davis, A.; Ruby, M. V.; Bergstrom, P. D. *Environ. Sci. Technol.* **1992**, *26* (3), 461–468.

(34) Ruby, M. V.; Davis, A.; Kempton, J. H.; Drexler, J. W.; Bergstrom, P. D. *Environ. Sci. Technol.* **1992**, *26* (6), 1242–1248.

(35) Chaney, R. L. U.S. Department of Agriculture, Beltsville, MD, personal communication, 1993.

(36) Miller, D. D.; Schricker, B. R. *Nutritional Bioavailability of Iron*; Kies, C., Ed.; American Chemical Society: Washington, DC, 1981.

(37) Allison, J. D.; Brown, D. S.; Novo-Gradac, K. J. *MINTEQA2/PRODEFA2, A Geochemical Assessment Model for Environmental Systems: Version 3.0 User's Manual*; Environmental Research Laboratory, Office of Research and Development, U.S. Environmental Protection Agency: Athens, GA, 1991.

(38) Mosimann, J. E. In *Handbook of Paleontological Techniques*; Kummel, B., Raup, D., Eds.; W. H. Freeman and Co.: San Francisco, CA, 1965; pp 636–673.